

Nonlocality Effect in Alpha Decay of Heavy and Superheavy Nuclei *

E. L. Medeiros¹, N. Teruya², S. B. Duarte¹, and O. A. P. Tavares¹

¹Centro Brasileiro de Pesquisas Físicas - CBPF/MCTI, Rua Dr. Xavier Sigaud 150, 22290-180, Rio de Janeiro - RJ, Brazil

²Departamento de Física, Universidade Federal da Paraíba -UFPB, Campus I, C. Postal 5008, 58051-970, João Pessoa - PB, Brazil.

July 29, 2022

Abstract

Alpha decay half-life of heavy and superheavy nuclei has been investigated using a potential barrier penetration model that adapts semiclassical WKB calculations to incorporate a coordinate-dependent effective mass for the alpha particle. This effect is a consequence of a dynamic property of nonlocality in the particle-nucleus interaction, as implemented in the barrier tunneling calculations of Ref. [1]. Calculations have been performed for a recent set of experimental data of 255 alpha-emitting nuclides, all selected with angular momentum $\ell = 0$ experimentally assigned. Results show a good agreement when compared to experimental half-life data, obtaining a standard deviation $\sigma = 0.306$, and fully satisfying the universal NUP and UDL systematics of alpha decay. Additionally, the present model has been applied to make half-life predictions for thirty-four possible, new alpha decay cases.

1 Introduction

Alpha emission has been an important topic of research in physics since the beginning of the era of radioactivity [2–4] and the consequent studies that led to the proposal of the nuclear atom [5, 6], passed through the first general laws of this type of nuclear emission [7] and evolved into the complex theories of quantum tunneling [8, 9].

Despite over a century of studies on this subject, a complete theory of α -decay still remains open. In recent decades, technological advances have allowed new experimental techniques to make more accurate measurements and discoveries of chemical elements with high atomic number [10–12], very unstable nuclei with exotic structure.

*In celebration of the 170th birth anniversary of Antoine-Henri Becquerel, the discoverer of radioactivity.

Currently, several α -decay models are applied to make predictions of decay chains in the mass region of superheavy nuclei, leveraging knowledge towards the limits of the production of nuclei of large atomic number [13]. In this context, evaluating the validity of universal systematics of decay in this region of superheavy mass may be a good indicator of the reliability of these studies.

In order to improve the theoretical results in relation to the experimental data, studies with different approaches on α decay, such as a more realistic nuclear potential to apply to this system, half-life calculations, universal systematics, decay chains, nuclear deformations, adjustments of preformation factors, analytical formulas to describe the α -decays, and other properties of heavy and superheavy nuclei have been reported in the literature [14–49].

In this work, we calculate alpha emission half-lives for a set of 255 experimental data covering a large mass region of heavy and superheavy nuclei ($52 \leq Z \leq 118$) and assigned angular momentum $\ell = 0$. Our theoretical model considers the nonlocality effect of the particle-nucleus interaction [1, 50–52] in a version of the WKB approximation [1], resulting in an effective alpha mass dependent on the radial coordinate tunneling through the potential barrier [1, 23]. The proposal that a global potential to represent the particle-nucleus interaction must be non-local in nature was launched in the late 1950s [53, 54]. In the version of a local potential representing the particle-nucleus interaction, an effective mass variable with the radial coordinate of the particle can be defined as a consequence of a velocity-dependent potential that expresses the nonlocality effect of the interaction [1, 50–52].

First, we apply the model to 239 α -emitters ($52 \leq Z \leq 103$), whose experimental measurements are more abundant and accurate. We then expanded the dataset by incorporating 16 more decays in the superheavy mass region ($104 \leq Z$), totaling 255 decays. Thus, we find that, in both cases, our calculations are in good agreement with the experimental data, satisfying the usual universal decay systematics (NUP [21] and UDL [20]) covering a large mass range of heavy and superheavy nuclei. After these successful checks, we applied the calculations to make predictions for thirty-four new α -decay cases with no experimental half-life data for the alpha channel, but only the total half-life.

2 Theoretical Model

2.1 Alpha-Cluster Potential Model

Alpha decay half-lives are calculated using the semi-classical WKB approximation with an implementation that considers a coordinate dependence on the particle mass. The application cases of our interest are those decays in the mass region of heavy and superheavy nuclei with strong experimental evidence of angular momentum $\ell = 0$, for which we have compiled a set of recent experimental data with 255 alpha emitters. In this context, considering only decay modes with zero angular momentum, Coulomb's interaction becomes the main contribution to produce the potential barrier for the quantum tunneling of the alpha particle. Despite that, in the vicinity of the diffuse nuclear radius, the nuclear potential well plays an important role to locating the internal return point and defining the rise of the barrier. Thus, the total potential is formed by

the superposition of the nuclear potential well (V_N) plus the Coulomb potential (V_C): $V(r) = V_N(r) + V_C(r)$.

The V_N potential was obtained from Ref. [15], in which the set of parameters was adjusted to give a good agreement with experimental data of half-lives and excitation energies for α -decay, covering a variety of light, medium and heavy nuclei: $V_0 = 220$ MeV; $\beta = 0.3$; $a = 0.65$ fm, and an improved nuclear radius taken from Ref. [39]:

$$V_N(r) = -V_0 \left\{ \frac{\beta}{1 + \exp(\frac{r-R}{a})} + \frac{1-\beta}{[1 + \exp(\frac{r-R}{3a})]^3} \right\}. \quad (1)$$

This nuclear potential was taken from the empirical adjustments made by Buck *et al.* [15]. They found that the cubic term, in addition to the usual format of the Woods-Saxon potential, led to a better fit of their alpha-cluster model in reproducing energy spectra and half-lives of nuclei for a large range of nuclear mass, from light to heavy nuclei [15].

As we only treat situations with zero angular momentum, the potential barrier is generated by the Coulomb potential with the α -particle interacting with a daughter nucleus treated as a uniformly charged sphere of radius R :

$$V_C(r) = \begin{cases} Z_\alpha Z_D e^2 [3 - (r/R)^2] / 2R & \text{for } r \leq R \\ Z_\alpha Z_D e^2 / r & \text{for } r > R \end{cases}. \quad (2)$$

2.2 Half-life calculation

The semi-classical WKB approach was applied to calculate the barrier penetrability factor P that determines the half-life (T):

$$T = \frac{\ln(2)}{FP}. \quad (3)$$

The F factor relates to the internal structure of the nucleus, giving a measure of the readiness rate for the alpha particle to initiate the escape through the penetration of the potential barrier. This factor accounts for the product between two usual parameters, namely, preformation S and assault rate λ_0 , $F = S\lambda_0$, as they were used in our previous work [23]:

$$\lambda_0 = \sqrt{\frac{Q - V_{\min}}{4\mu(R_2 - R_1)^2}}, \quad (4)$$

and the S values given in Ref. [25]: $S_{\text{odd-odd}} = 0.15$, $S_{\text{A-odd}} = 0.21$, and $S_{\text{even-even}} = 0.34$. The barrier penetrability P is defined as the usual form, with the alpha particle tunneling the barrier between the two classical turning points R_2 and R_3 (radial coordinates at which $V(r) = Q$, with $Q = Q_\alpha$; see Figs. 1c and 1b):

$$P = \exp\left(-\frac{2}{\hbar} \int_{R_2}^{R_3} \sqrt{2\mu(V - Q)} dr\right). \quad (5)$$

In the Eqs. 4 and 5 above, R_1 is the innermost classical turning point within the potential well ($R_1 = 0$ in cases with $\ell = 0$), the particle oscillates between R_1 and R_2

in the assault on the barrier, μ is the reduced mass of the α -daughter nucleus system, V_{min} is the minimum value of the potential well [23] and the Q -value was calculated as reported in Ref. [41] with the recent atomic mass excess given in Ref. [10].

2.3 Nonlocality Effect

In the present study, the difference from our previous calculations [23] is due to a redefinition of the reduced mass μ of the system, now including an effective mass m^* for the alpha particle:

$$\mu = \frac{m^* M}{m^* + M}, \quad (6)$$

where M is the nuclear (rather than atomic) mass of the daughter nucleus. The modification implemented here in the effective mass considers a dynamic effect of nonlocality, intrinsic to the particle-nucleus interaction, whose effect can be incorporated by making a mass dependent on coordinates [1, 50–52]:

$$m^* = \frac{m}{1 - \rho(r)}, \quad (7)$$

where m is the free mass of α particle and the $\rho(r)$ function is defined in [1, 50–52]:

$$\rho(r) = \rho_S a_S \frac{d}{dr} \left[1 + \exp \left(\frac{r - R_S}{a_S} \right) \right]^{-1}. \quad (8)$$

The R_S parameter is defined as $R_S = R + \Delta R$, giving the centroid location of the effective mass function ρ ; a_S is related to the width of this function. We take the values $a_S = a$ and R defined as in nuclear potential V_N ; $\Delta R = 3.44$ fm was adjusted keeping a very close connection with the α -radius experimental data ($\Delta R = 2R_\alpha$). The mass parameter ρ_S was adjusted globally for the entire set of experimental data (see Section 3). In Ref. [1] we showed that the nonlocality effect can be introduced as a dynamic contribution represented by an energy-dependent term in the particle-nucleus interaction. Anyway, this implementation in the WKB calculations keeps the penetrability factor P in the same form as the one with constant mass during the quantum tunneling. In practical terms, this adjustment occurs consistently only by exchanging the free mass m for its effective counterpart m^* in the reduced mass μ [1]. To illustrate the contribution of effective mass m^* to the tunneling calculations, Fig. 1 shows the functions for the reduced effective mass μ (Fig. 1a), the components V_N and V_C of the potential, Q_α -value (Fig. 1b) and the function $f(r) = \sqrt{\mu(V - Q)}$ within the integrand in the barrier penetrability P (Eq. 5) for the case of α -decay of ^{185m}Pt (Fig. 1c). It is observed that the nonlocality effect produces a pronounced contribution on the reduced effective mass in the region around the nuclear surface (Fig. 1a), modifying the penetrability integrand function in relation to the standard calculation considering the free mass of the alpha particle (Fig. 1c).

3 Results

Firstly, we compiled a set of alpha emitters with accurate half-life measurements, all selected with predominantly *zero* angular momentum decays. These experimental data

were compiled from recent publications [10]. The dataset covers a wide region of nuclear mass, divided into two atomic number groups: 239 heavy nuclei with $52 \leq Z \leq 103$ and 16 superheavy nuclei with $104 \leq Z \leq 118$, totalizing 255 emitting nuclei (heavy and superheavy). The parameter ρ_S in the half-life calculations of the dataset was adjusted to minimize the standard deviation $\sigma_{n-\rho_S}$:

$$\sigma_{n-\rho_S} = \left\{ \frac{1}{n-1} \sum_{i=1}^n (\Delta\tau_i)^2 \right\}^{1/2}; \quad \Delta\tau_i = \log_{10}(T_i^{\text{cal}}) - \log_{10}(T_i^{\text{exp}}), \quad (9)$$

where T_i^{cal} and T_i^{exp} are the calculated and experimental half-lives of the i -th decaying nucleus, respectively, and $\Delta\tau_i$ measures the logarithmic deviation between calculated and experimental data. At this point, for a measure of the contribution of the nonlocality effect on the half-life results, it is worth mentioning that in the previous work [23], with no nonlocality effect ($\rho_S = 0$) and $n = 164$ decay cases with $51 \leq Z \leq 103$, a standard deviation $\sigma_{164_0} = 0.36$ was obtained (the subscript 164_0 in the notation σ_{164_0} refers to $n = 164$ and $\rho_S = 0$; this type of notation will be used later in the text). In current calculations, we consider the group of heavy nuclei ($n = 239$) first. The best results for the calculated half-lives, in comparison with the experimental data, were obtained through an adjustment with $\rho_S = -0.366$, which provided a minimum standard deviation $\sigma_{239_{-0.366}} = 0.312$. This result shows a significant improvement over our previous work with $\sigma_{164_0} = 0.36$ [23], further emphasizing that now the number of decay cases has increased by approximately 46%. It is noteworthy that in the current theoretical formulation the distances between the calculated and experimental values ($\Delta\tau_i$) have decreased in relation to the previous results with σ_{164_0} , although the number of studied cases has increased considerably. In a second step, now considering the larger dataset with $n = 255$ heavy and superheavy emitters and making only a small adjustment of $\rho_S = -0.375$, we can still get good results obtaining $\sigma_{255_{-0.375}} = 0.306$, which is a little better than the previous value $\sigma_{239_{-0.366}} = 0.312$, or a good improvement over the case without the nonlocality effect, $\rho_S = 0$, resulting in $\sigma_{255_0} = 0.352$. These results are summarized in Table 1.

Table 1: Global ρ_S adjustments for both sets of alpha emitters $n = 239$ (heavy nuclei) and $n = 255$ (heavy and superheavy nuclei). The ρ_S parameter is adjusted to minimize the standard deviation $\sigma_{n-\rho_S}$ and, in addition, to centralize at zero the $\Delta\tau_i$ distribution of the logarithmic deviations of the calculated half-lives from the experimental ones.

n	ρ_S	$\sigma_{n-\rho_S}$	$\Delta\tau$
239	-0.366	0.312	0
255	-0.375	0.306	0
255	0	0.352	-0.18

Although the results in Table 1 show that the standard deviation $\sigma_{n-\rho_S}$ is a little better for the adjustments considering the ρ_S parameter, the nonlocality effect has an additional contribution on the results, as we can see in Fig. 2. This figure shows the distribution of deviations $\Delta\tau_i$, for $n = 255$ group, through two types of calculation to illustrate the effect of the contribution of nonlocality in these calculations. Fig. 2a presents the deviations $\Delta\tau_i$ with $\rho_S = 0$, where we can see that the centroid $\Delta\tau = -0.18$ of the distribution is shifted to negative values of $\Delta\tau_i$. In this case, most of the

calculated half-lives are smaller than the experimental values, which is an indication that some additional contribution to the previous theoretical model ($\rho_S = 0$) needs to be considered. On the other hand, the centroid is shifted to $\Delta\tau = 0$ when the nonlocality effect is considered in the decay calculations using the adjusted value of $\rho_S = -0.375$ in Fig. 2b.

At this point, it is important to note that a consequence of the dynamic effect of the nonlocality of the potential is to produce an increase of the reduced effective mass of the alpha particle, having an increased peak value of approximately 10% at the radial coordinate $r = R_S$, in the case for α -decay of ^{185m}Pt isotope, which directly influences the results in relation to the model with the free mass of the particle (see Fig. 1).

3.1 Universal Systematics

In addition to comparing the minimization of the standard deviation $\sigma_{255-0.375} = 0.306$, the confidence of our results was also tested in two forms of universal systematics, namely, NUP (New Universal Plot [21]) and UDL (Universal Decay Law [20]). Fig. 3 shows the NUP systematics by comparing our results with experimental data for heavy and superheavy nuclei. This systematics is a useful way of interpreting the results of the set of half-lives calculated by Eq. 3: $\log_{10} T = -a \log_{10} P - \log_{10} S + c$. The fitting parameters of this straight-line are given in Table 2.

Table 2: NUP-systematics parameters for heavy and superheavy nuclei.

Ref.	n α -emitters	ρ_S	a	c	$\sigma_{n-\rho_S}$
Present work	255 ($52 \leq Z \leq 118$)	-0.375	1.0	-21.7631	0.306
[23]	164 ($51 \leq Z \leq 103$)	-	1.0	-21.7615	0.360
[21]	163 (+27 clusters)	-	1.0	-22.16917	0.428

On the other hand, the UDL systematics [20] is presented in Fig. 4. The Y function is defined as: $Y = \log_{10} T - b\vartheta = a\chi + c$, where a , b and c are adjustable values, $\vartheta = \sqrt{A_r Z_\alpha Z_D (A_\alpha^{1/3} + A_D^{1/3})}$ with $A_r = \frac{A_\alpha A_D}{A_\alpha + A_D}$, variable $\chi = (Z_\alpha Z_D) \sqrt{\frac{A_r}{Q}}$ and the half-life T should be expressed in second. In Table 3 is showed the parameters of UDL systematics in comparison with the others adjusted in our previous work.

Table 3: Parameters adjusted in the UDL systematics for 255 α -emitters, heavy and superheavy nuclei, minimizing the standard deviation $\sigma_{n-\rho_S}$ (Table 1).

Ref.	n	a	b	c	$\sigma_{n-\rho_S}$	ρ_S
Present work	255	0.4174	-0.4175	-22.949	0.306	-0.375
Present work	239	0.4175	-0.4182	-22.920	0.312	-0.366
[23]	164	0.4171	-0.4311	-22.364	0.360	-
[20]		0.4065	-0.4311	-20.7889	0.3436	-

The data presented in Fig. 4a show that the results of our calculations, using the parameters in Table 3, are perfectly well represented by the UDL systematics, while the experimental data suffer a small deviation from the UDL (see Fig. 4b), which, equally, also happens in relation to our results (Fig. 4c and Table 3).

4 Predictions for some unknown alpha-decay emitter channels

After some successful tests of comparing our model results with known experimental data, we can apply these calculations to make predictions of some α -decay cases that do not yet have experimental data for this specific channel, but only for the total half-lives. In this way, we found a set of thirty-four possible new α -decay cases with zero angular momentum, for which the experimental total half-life is known, but not the α -channel branching ratio. The results are shown in Table 4.

Next, in Fig. 5 we present the results of the predictions superimposed on the graph of the UDL systematics showed in Fig. 4a, in which we can also observe a good agreement between our calculations with this systematics, noting that the experimental data from predictions are not placed in this figure because only their total half-lives are known.

5 Concluding remarks

The calculations certify our previous results [23] that the α -decay for heavy and superheavy nuclei can together satisfy the same universal systematics, a powerful tool that can allow good predictions of half-lives or new α -decay chains. Furthermore, the inclusion of the nonlocality effect of the particle-nucleus interaction produces a better adjustment of the mean field potential in the calculations and, therefore, presents an important contribution in the sense of minimizing the deviations between the theoretical and experimental results, making them closer and more centralized. On this opportunity, encouraged by the good fits between the results of our theoretical model and the experimental data, we have expanded the calculations to make half-life predictions for thirty-four new possible α -emitters.

References

- [1] N. Teruya, S. B. Duarte and M. M. N. Rodrigues, Phys. Rev. C **93**, 024606 (2016).
- [2] A.-H. Becquerel, Comptes Rendus **122**, 420 (1896).
- [3] M. P. Curie and S. Curie, Comptes Rendus **127**, 175 (1898).
- [4] E. Rutherford, Phil. Mag. **47**, 109 (1899).
- [5] H. Geiger, and E. Marsden, Proc. Roy. Soc. A **82**, 495 (1909).
- [6] E. Rutherford, Phil. Mag. **21**, 669 (1911).
- [7] H. Geiger, and J. M. Nuttall, Phil. Mag. **22**, 613 (1911).
- [8] G. Gamow, Z. Phys. **51**, 204 (1928).
- [9] R. Gurney, and E. Condon, Nature **122**, 439 (1928).
- [10] M. Wang et al., Chinese Phys. C **45**, 030003 (2021).
- [11] F. G. Kondev, et al., Chinese Phys. C **45**, 030001 (2021).
- [12] M. L. Terranova and O. A. P. Tavares, Rend. Fis. Acc. Lincei (2022) doi.org/10.1007/s12210-01057-w.
- [13] S. A. Seyydi, Mod. Phys. Lett. A **36**, 2150033 (2021).
- [14] H. Buck, A. C. Merchant, and S. M. Perez, Phys. Rev. C **45**, 2247 (1992).
- [15] H. Buck, A. C. Merchant, and S. M. Perez, Phys. Rev. C **51**, 559 (1995).
- [16] M. Goncalves, S.B. Duarte, Phys. Rev. C **48**, 2409 (1993).
- [17] S. B. Duarte, O. A. P. Tavares, F. Guzman, A. Dimarco, F. Garcia, O. Rodriguez and M. Goncalves, At. Data Nucl. Data Tables **80**, 235 (2002).
- [18] B. Alex Brown, Phys. Rev. C **46**, 811 (1992).
- [19] C. Qi, F. R. Xu, R. J. Liotta, and R. Wyss, Phys. Rev. Lett. **103**, 072501 (2009).
- [20] C. Qi, F. R. Xu, R. J. Liotta, R. Wyss, M. Y. Zhang, C. Asawatangtrakuldee and D. Hu, Phys. Rev. C **80**, 044326 (2009).
- [21] D. N. Poenaru, R. A. Gherghescu, and W. Greiner, Phys. Rev. C **83**, 014601 (2011).
- [22] M. A. Souza and H. Miyake, AIP Conf. Proc. **1351**, 77 (2011).
- [23] S. B. Duarte, and N. Teruya, Phys. Rev. C **85** 017601 (2012).
- [24] V. Y. Denisov and A. A. Khudenko, Phys. Rev. C **79**, 054614 (2009).
- [25] Y. Qian, Z. Ren, and Dongdong Ni, Phys. Rev. C **83**, 044317 (2011).

- [26] Dongdong Ni, and Z. Ren, Phys. Rev. C **83**, 067302 (2011).
- [27] K. P. Santhosh, B. Priyanka, J. G. Joseph, and S. Sahadevan, Phys. Rev. C **84**, 024609 (2011).
- [28] M. R. Pahlavani, S. A. Alavi, and N. Tahanipour, Mod. Phys. Lett. A **28**, 1350065 (2013).
- [29] M. Ismail and A. Adel, Phys. Rev. C **88**, 054604 (2013).
- [30] T. T. Ibrahim, and S. M. Wyngaardt, J. Phys. G: Nucl. Part. Phys. **41** 055111 (2014).
- [31] K.P.Santhosh, A.Augustine, C.Nithya, B.Priyanka, Nucl. Phys. A **951**, 116 (2016).
- [32] A.I.Budaca, R.Budaca, I.Silisteanu, Nucl. Phys. A **951**, 60 (2016).
- [33] K. P. Santhosh, C. Nithya, H. Hassanabadi, D. T. Akrawy, Phys. Rev. C **98**, 024625 (2018).
- [34] V. Dehghani, S. A. Alavi, and Kh. Benam, Mod. Phys. Lett. A **33**, 1850080 (2018).
- [35] A. Daei-Ataollah, O. N. Ghodsi, and M. Mahdavi, Phys. Rev C **97**, 054621 (2018).
- [36] T. L. Zhao , X. J. Bao and S. Q. Guo, J. Phys. G: Nucl. Part. Phys. **45**, 025106 (2018).
- [37] T. L. Zhao, and X. J. Bao, Phys. Rev. C **98**, 064307 (2018).
- [38] S. S. Hosseini, H. Hassanabadi and Dashty T. Akrawy, Mod. Phys. Lett. A **34**, 1950039 (2019).
- [39] O. A. P. Tavares, E. L. Medeiros, and M. L. Terranova, Appl. Radiat. and Isot. **166**, 109381 (2020).
- [40] P. Moller, J.R. Nix, W.D. Myers, and W.J. Swiatecki, Atom. Data Nucl. Data Tables **59**, 185 (1995).
- [41] O. A. P. Tavares, E. L. Medeiros, and M. L. Terranova, Mod. Phys. Lett. A **36**, 2150036 (2021).
- [42] M. Hosseini-Tabatabaei, S. A. Alavi, V. Dehghaniy, Can. Jour. of Phys., **99**, 24 (2021).
- [43] Na-Na Ma, X. J. Bao, H. F. Zhang, Chin. Phys. C **45**, 024105 (2021).
- [44] J. P. Cui, Y. H. Gao, Y. Z. Wang, and J. Z. Gu, Nucl. Phys. A **1017**, 122341 (2022).
- [45] Z. Yuan, D. Bai, Z. Ren, and Z. Wang, Chin. Phys. C **46**, 024101 (2022).

- [46] C. He, Z. M. Niu, X. J. Bao, and J. Y. Guo, *Chin. Phys. C* **46**, 054102 (2022).
- [47] D. T. Akrawy, H. Hassanabadi, S. S. Hosseini, and K. P. Santhosh, *Nucl. Phys. A* **971**, 130 (2018).
- [48] J.-G. Deng, H.-F. Zhang, and G. Royer, *Phys. Rev. C* **101**, 034307 (2020).
- [49] G. Royer, *Nucl. Phys. A* **848**, 279 (2010).
- [50] M. I. Jaghoub, M. F. Hassan, and G. H. Rawitscher, *Phys. Rev. C* **84**, 034618 (2011).
- [51] R. A. Zureikat and M. I. Jaghoub, *Nucl. Phys. A* **916**, 183 (2013).
- [52] S. Alameer, M. I. Jaghoub, and I Ghabar, *J. Phys. G: Nucl. Part. Phys.* **49**, 015106 (2022).
- [53] H. Feshbach, *Annu. Rev. Nucl. Sci.* **8**, 49 (1958).
- [54] W. E. Frahn and R. H. Lemmer, *Il Nuovo Cimento* **5**, 1564 (1957).

Table 4: Prediction for thirty-four new cases of $\ell = 0$ α -emitting nuclei: the total half-lives in column 4 are experimental data from Ref. [11], and the α half-lives in column 5 have been calculated by using the model of the present work with $\rho_S = -0.375$, this parameter value being obtained from the half-life data of 255 heavy and superheavy α -emitters (see Table 1).

i	Z	A	$T_{\text{tot}}^{\text{exp}}$ (s)	T_{α}^{calc} (s)
1	52	110	1.86×10^1	1.28×10^6
2	69	155	4.50×10^1	3.83×10^3
3	71	157	7.70×10^0	1.19×10^2
4	73	161	3.00×10^0	1.74×10^2
5	73	163	1.06×10^1	5.60×10^4
6	75	161	4.40×10^{-4}	4.09×10^{-2}
7	75	167	5.90×10^0	2.33×10^2
8	77	165	5.00×10^{-8}	4.89×10^{-3}
9	79	169	1.50×10^{-4}	4.63×10^{-4}
10	79	171	2.23×10^{-5}	3.77×10^{-3}
11	81	183	6.90×10^0	3.27×10^2
12	92	220	6.00×10^{-8}	7.97×10^{-8}
13	92	236	1.20×10^{-7}	9.25×10^0
14	94	224	1.00×10^{-5}	3.47×10^{-6} *
15	96	232	1.00×10^1	1.17×10^1
16	96	250	2.62×10^{11}	2.07×10^{13}
17	100	242	8.00×10^{-4}	3.66×10^{-1}
18	100	244	3.12×10^{-3}	9.65×10^{-1}
19	102	258	1.23×10^{-3}	7.33×10^1
20	103	257	2.70×10^{-1}	1.71×10^{-1} *
21	104	260	2.10×10^{-2}	1.45×10^0
22	104	264	3.60×10^3	9.56×10^2 *
23	104	266	1.44×10^4	3.77×10^4
24	105	257	6.70×10^{-1}	3.65×10^{-1} *
25	106	258	2.70×10^{-3}	4.99×10^{-2}
26	106	262	1.03×10^{-2}	6.57×10^{-2}
27	106	264	7.80×10^{-2}	8.22×10^{-1}
28	106	268	1.20×10^2	6.41×10^2
29	108	274	5.00×10^{-1}	3.01×10^{-1} *
30	108	276	1.00×10^{-1}	2.30×10^0
31	112	278	2.00×10^{-3}	2.98×10^{-4} *
32	112	280	5.00×10^{-3}	5.32×10^{-3}
33	112	282	1.10×10^{-3}	1.28×10^{-1}
34	114	284	3.10×10^{-3}	2.09×10^{-2}

*Case for which α -branching ratio > 1 . Roughly 18% of the cases listed fall into this category; they have been kept to allow for the possibility of uncertainties in the data and calculations.

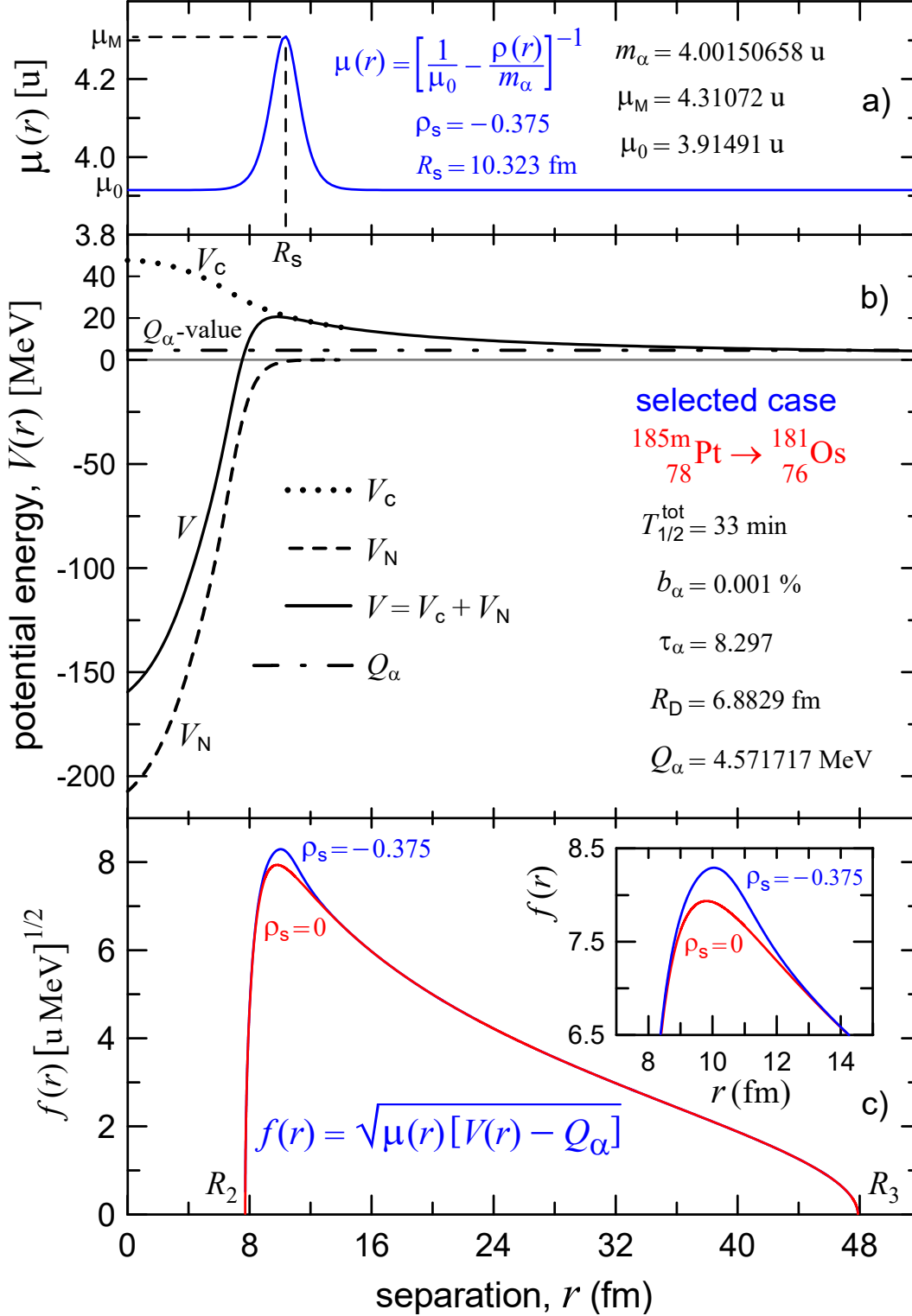


Figure 1: The contribution of the nonlocal effect on tunneling calculations. Selected example for α -decay from $^{185}_{78}\text{Pt}$: (a) effective reduced mass μ considering nonlocality effect with $\rho_s = -0.375$; (b) components of the potential: nuclear V_N , Coulomb V_C , Total V , and Q -value; (c) comparison between the functions $f(r)$ in the integrand of the barrier penetrability: considering the reduced masses μ (blue line, $\rho_s = -0.375$) and μ_0 (red line, $\rho_s = 0$).

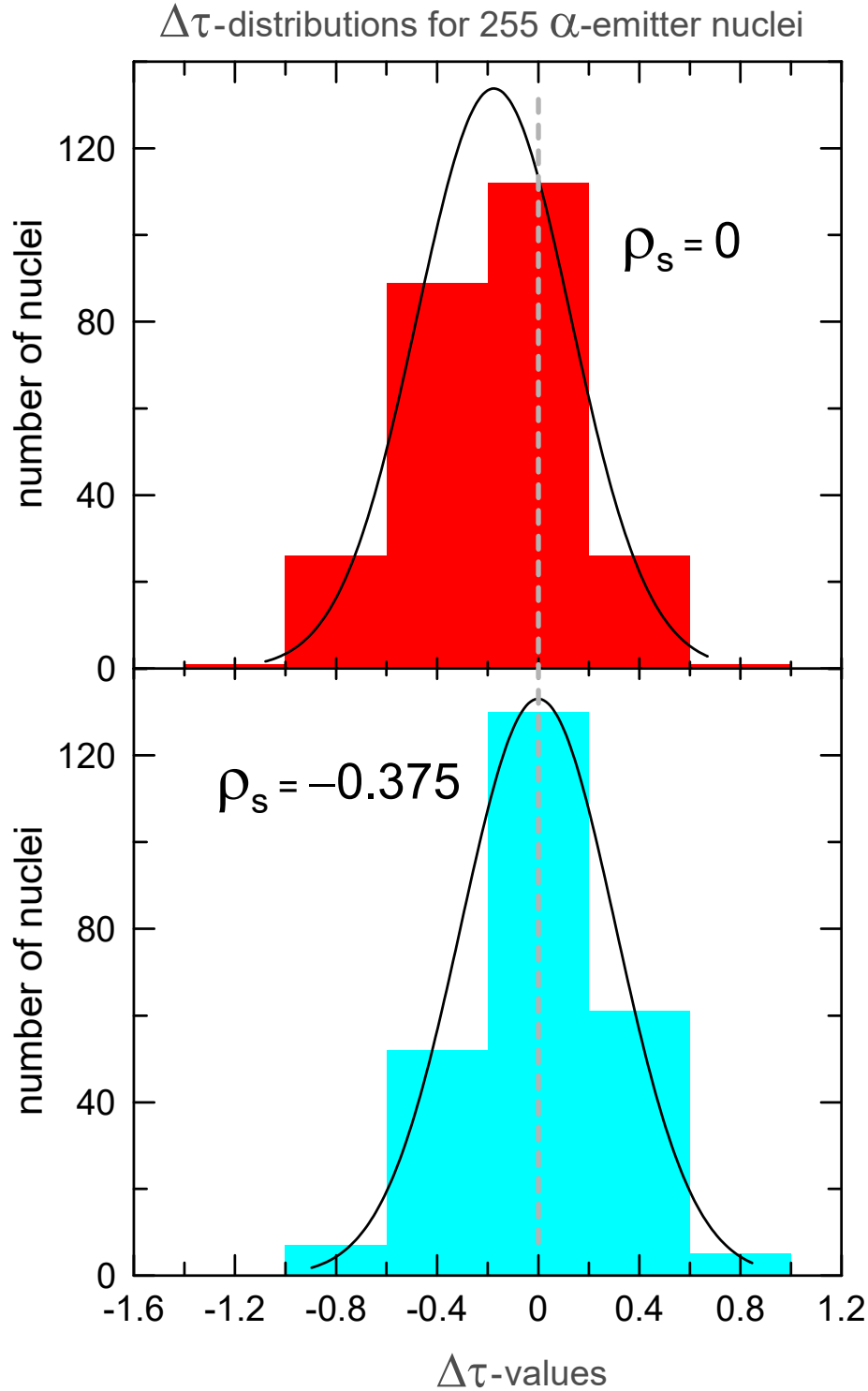


Figure 2: $\Delta\tau$ -distributions for 255 α -emitters. (a) Results for the calculations with $\rho_s = 0$ (without nonlocality effect). In this case, most of the calculated half-lives are smaller than the experimental values, which can be observed with the centroid being shifted to the negative value $\Delta\tau = -0.180$. (b) However, the centroid is exactly on $\Delta\tau = 0$ when the nonlocality effect is considered in the calculations with $\rho_s = -0.375$.

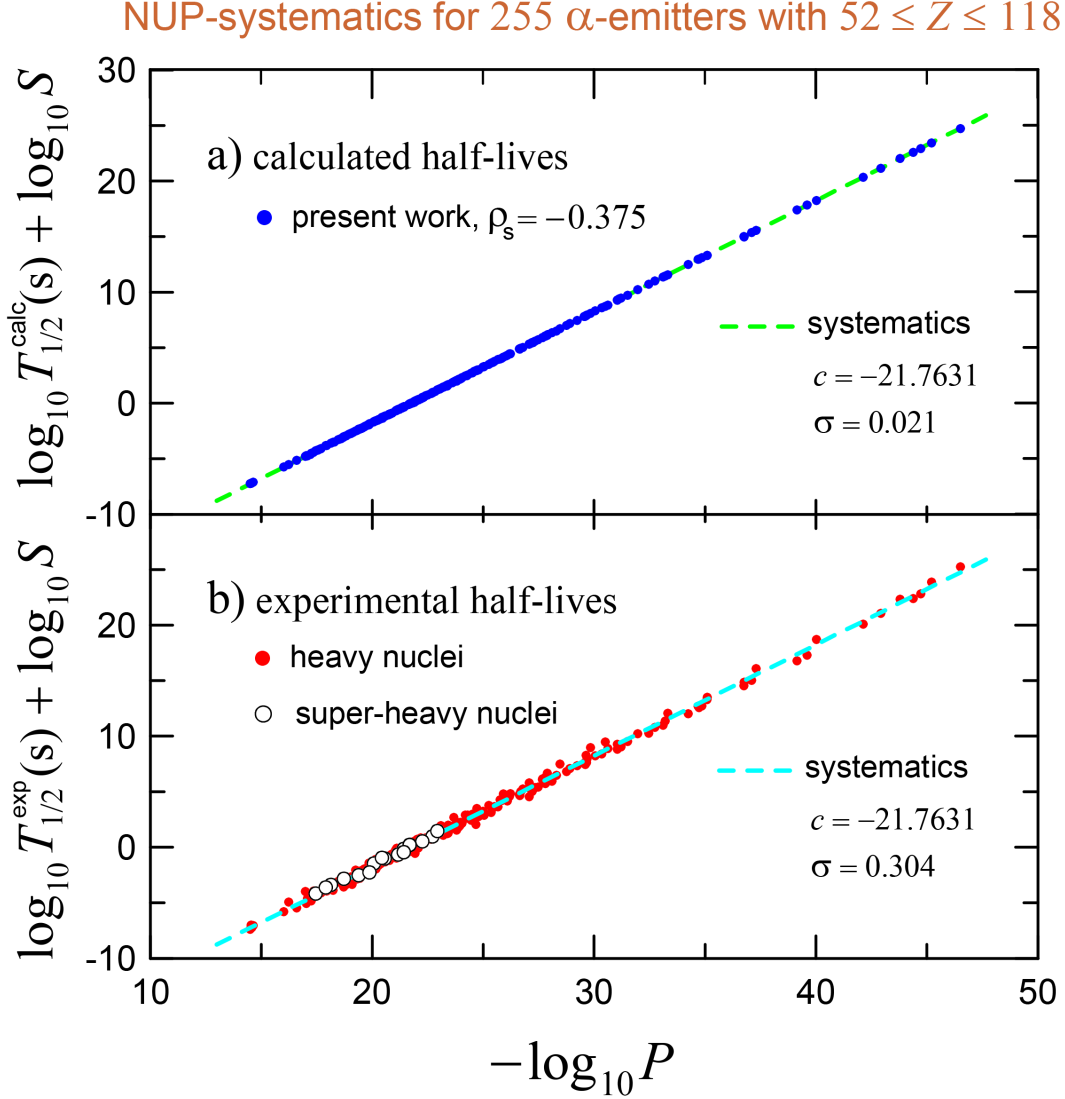


Figure 3: NUP systematics for 255 heavy and superheavy α -emitters nuclei with $52 \leq Z \leq 118$: (a) theoretical results with $\rho_s = -0.375$ (for all decay cases shown in Fig. 2b); (b) the experimental data are displayed on the fitted NUP straight line from part-a. The σ -value in parts a and b measures the standard deviation of the data from the straight line in part-a. The theoretical results are well adjusted on the NUP line ($\sigma = 0.021$), while the experimental ones show a small deviation ($\sigma = 0.304$).

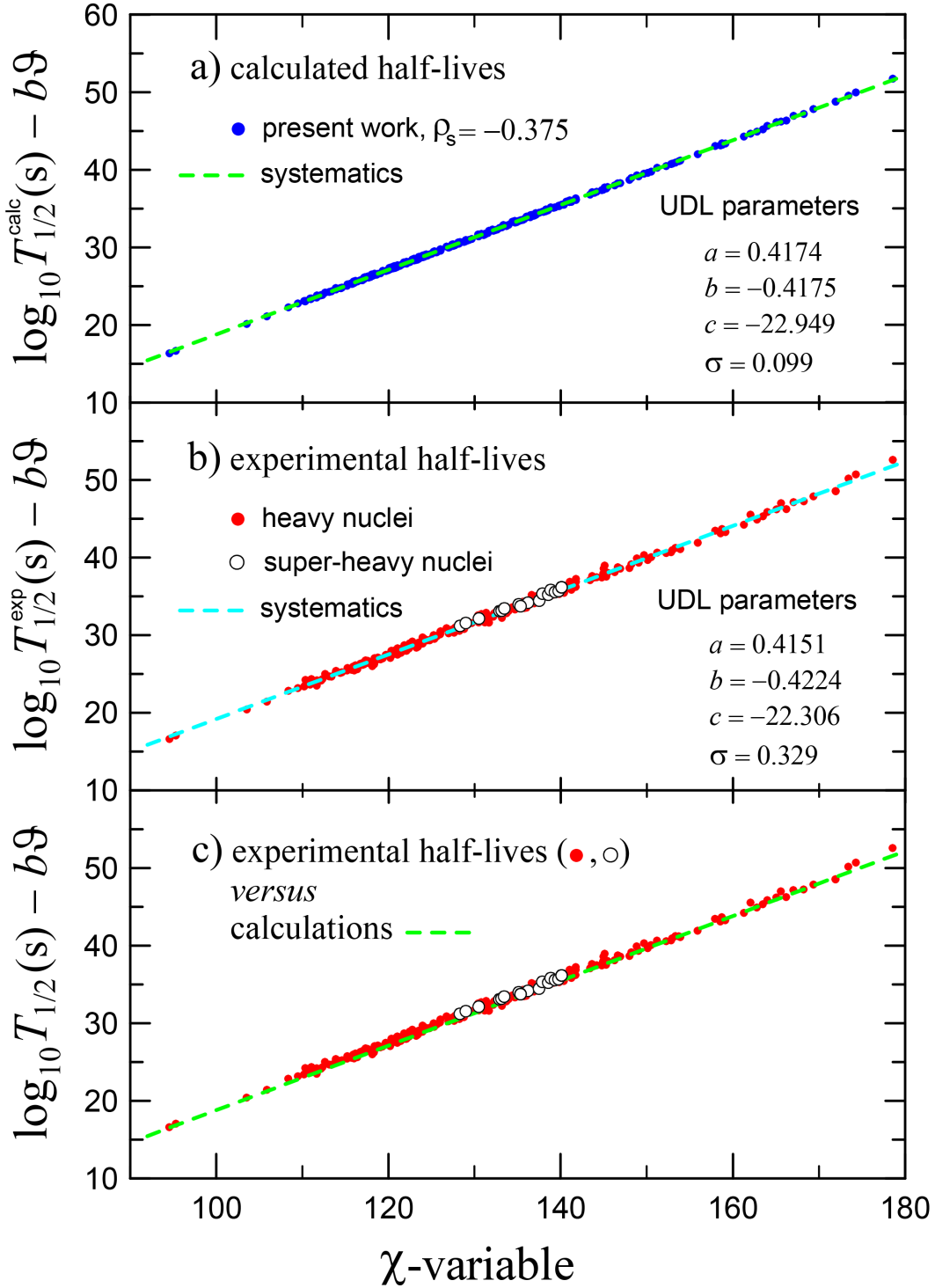
UDL-systematics for 255 α -emitters with $52 \leq Z \leq 118$ 

Figure 4: The UDL systematics for 255 α -emitters with the parameters given in Table 3. (a) The UDL systematics (dashed green line) adjusted for our theoretical results (blue dots); (b) UDL systematics (dashed blue line) adjusted for experimental half-lives (blue dots and white dots); (c) the experimental data (blue dots and white dots in Fig. 4b) are superimposed on the dashed green line of the adjusted theoretical UDL (Fig. 4a). The σ -value in parts a and b measures the standard deviation of the data from the UDL straight line. The theoretical results are well adjusted on the UDL line ($\sigma = 0.099$), while the experimental ones show a small deviation ($\sigma = 0.329$).

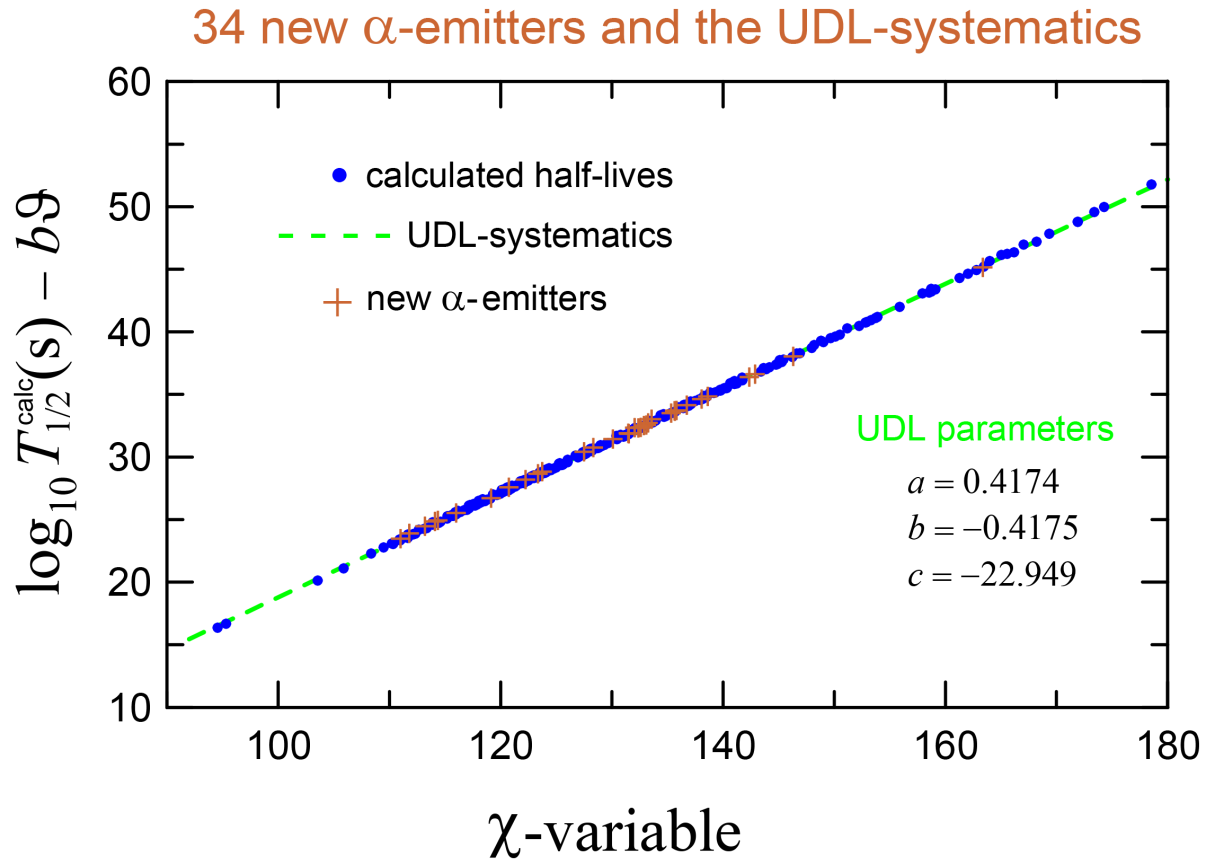


Figure 5: Half-life predictions of thirty-four new α -emitters are displayed by overlaying the same UDL systematic in Fig. 4a. It is observed that the prediction cases follow the same line adjusted previously for the 255 decays with the known alpha half-life experimental data. These new results are shown in Table 4.